

# OBSERVATION AND ANALYSIS OF POLAR MESOSPHERIC WINTER ECHOES MODULATED BY ARTIFICIAL ELECTRON HEATING

O. Havnes<sup>1,2,3</sup>, C. La Hoz<sup>1</sup>, M.T. Rietveld<sup>4</sup>, M. Kassa<sup>1,2</sup>, G. Baroni<sup>1</sup> and A. Biebricher<sup>1</sup>

<sup>1</sup>*Institute of Physics and Technology, University of Tromsø, Tromsø, Norway, Email: [ove.havnes@uit.no](mailto:ove.havnes@uit.no), [cesar.la.hoz@uit.no](mailto:cesar.la.hoz@uit.no), [meseret-kassa.bekele@uit.no](mailto:meseret-kassa.bekele@uit.no), [baroni\\_60@hotmail.com](mailto:baroni_60@hotmail.com), [alexander.biebricher@uit.no](mailto:alexander.biebricher@uit.no).*

<sup>2</sup>*Max-Planck-Institute für extraterrestrische Physik, D-85741 Garching, Germany*

<sup>3</sup>*University Centre at Svalbard (UNIS), Longyearbyen, Norway.*

<sup>4</sup>*EISCAT, Ramfjordbotn, Norway, Email: [mike@eiscat.uit.no](mailto:mike@eiscat.uit.no).*

## ABSTRACT

Observations and analysis of Polar Mesospheric Winter Echoes (PMWE) modulated by the EISCAT Heating Facility are presented. The PMWE were observed with a collocated new 56 MHz radar (MORRO). The analysis is based on that small dust particles are present in the PMWE. The increase in electron temperature when the heating was switched on, measured by its effect on the PMWE signal, was found to be up by a factor 3-3.5. The height profile of the heating agree with model heating calculations and a high electron density in the PMWE region consistent with that the PMWEs were observed during disturbed magnetospheric conditions. Deviations from the theoretical curve indicate that in some regions the dust density is large enough to reduce the electron density substantially. The PMWE show small but clear overshoot effects indicating small nanometer sized dust particles.

## 1. INTRODUCTION

The usefulness of applying artificial electron heating [1] to mesospheric phenomena has been convincingly demonstrated by the observations of its effect on the Polar Mesospheric Summer Echoes (PMSE). Reference [2] showed that with a sequence of equal and short (10-20 sec) heater on and off time intervals, one could get a situation where the PMSE was severely weakened when the heater was on, and where it returned to its initial value as the heater was switched off. References [3,4] showed that another heater on and off sequenced could give rise to a PMSE overshoot phenomena where the PMSE backscatter, being reduced in intensity as the heater was switched on, could when the heater was switched off, nearly instantaneously increase (overshoot) to a value up to 6-7 times that of the value before the heater was switched on. The shape of the backscatter intensity profile during a heater on/off overshoot cycle (OCC) contains information on the dust and plasma (dusty plasma) conditions and can be used as a dusty plasma diagnostic [5,6,7]

The PMWE is also affected by artificial electron heating as have been showed in several recent experiments [8,9,10,11]. However, the PMWE signal is very weak compared to PMSE. Typically strong PMWE layers are a factor  $10^4$  weaker than strong PMSE at 53.5 Mhz [12] and is very much affected by noise. At higher frequencies such as the EISCAT VHF (224 MHz) the PMWE signal is normally much weaker than at  $\sim 50$  MHz, as it also is for PMSE. Reference [7] showed that the early reported observations of heater effects on PMWE at VHF (224 MHz) [8,9] could not be interpreted in a consistent way and that no definite conclusions on PMWE conditions based on a dust overshoot model [5,6] could be drawn from those observations.

Reference [11] model PMWE variations observed with the EISCAT VHF antenna, where the PMWE was acted upon by the heater run with a 6 sec on and 6 sec off cycle, by a varying electron density due to an increased formation of negative ions when the electrons are heated. They find that the electron density could decrease to  $\sim 70$  % of that without heating. With their model for PMWE strength variation being proportional to the square of the electron density they get a decrease in strength from 1 to 0.5. Reference [10] found that the reduction in PMWE strength when the heater was switched on could be down to a factor 0.1 or less of the pre-heating value. We will later in the present paper show that such large reductions often occur. The heating used by [11] for the electrons is also probably too high. As is evident from the observations of [10], and in this paper the PMWE variations at 56 MHz as the heater is switched on or off is mainly characterized by a rapid reduction or increase of signal strength, and not the gradual transitions which the negative ion model predicts. Although the observations on which the analysis of [11] was based on was at 224 MHz we find that this demonstrate that the influence of negative ion production cannot be a dominant effect.

## 2. OBSERVATIONS

The observations of the heating effect on PMWE by [10], are the first overshoot observations of PMWE at low MST radar frequency. Reference [10] report from

observations on the 11<sup>th</sup> February 2008 where the heater was run in cycles of 20 sec on and 100 sec off. Although many layers of PMWE were present over a period of 7 hours, the layers were weak and not much above the noise level. They selected the strongest layer which remained reasonably stable over a period of 44 min. They observed that strong and rapid reductions of the signal down to .09 of the initial signal took place, followed by small but consistent overshoots of only  $\sim 1.1$  of the pre-heating PMWE strength. Reference [7] analyzed the averaged PMWE overshoot curve (OCC) of [10] and found that with a temperature increase of around a factor 5 when the heater is switched on, the curves could be reasonably well reproduced with a dust radius of around 3 nm. We will later show that the real heating factor should probably be somewhat lower, which indicate that the active dust particles in forming the overshoots should be slightly larger than 3 nm. The weak signals and limited height distribution of the strongest layers prevented [10] from analyzing height variations and time variations of heating and overshoot. In the following we will do this by analyzing PMWE observations from the 12<sup>th</sup> of February 2008 where strong PMWE was present. The heater cycling was 20 sec on and 100 sec off and several strong layers, extending over heights from 59.5 to 67 km, were present over a period of  $\sim 2.3$  hours. The PMWE as function of height and heater cycle (time) is shown in Fig.1. The maximum intensity in the layer is about one order of magnitude larger than the layer which [10] considered.

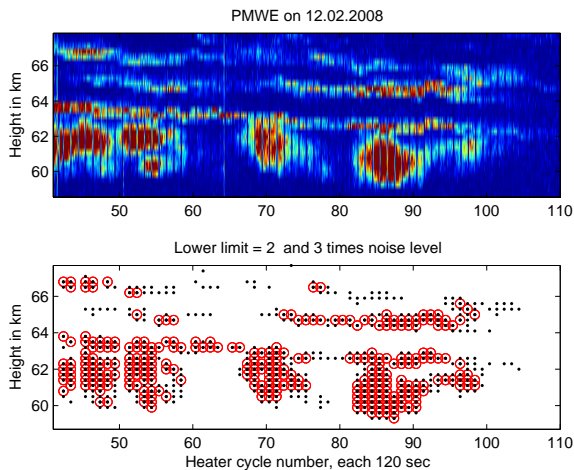


Fig.1. The upper part show the PMWE layer over 70 heater cycles each of 2 min and over a height range from 59 to 67.7 km height. The lower figure shows points where  $(S+N)/N > 2$  as black dots and  $> 3$  as red circles.

### 3. THEORETICAL HEATING CURVES AND COMPARISON WITH THE OBSERVED HEATING.

The heating effect caused by the transmission of high power transmission of electromagnetic waves, typically between 4 to 8 MHz [1], has been calculated in several papers [13,14,15]. The heating height profile for a given heater transmission power, depends critically on the electron density height profile. In Fig.2 we show the heating factor  $T_{e,hot}/T_N$ , which is the ratio of the heated electron temperature, to the unheated electron temperature (which is equal to the neutral and ion temperature which both are unaffected by the heater).

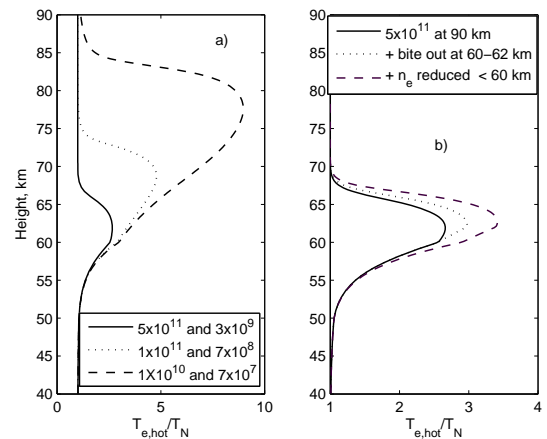


Fig. 2. In Fig 2a we show three examples of electron heating as a function of height. The electron density, assumed to decrease exponentially downward from 90 km with a scale height 5 km, have densities from  $10^{10}$  to  $5 \times 10^{11} \text{ m}^{-3}$  at 90 km. The corresponding electron densities at 65 km are given on the right hand side in the box. In Fig.2b we have focussed on the electron density profile with maximum within the PMWE layers (full line), and showed how changes in the electron densities within and below the PMWE layer can affect the heating profile. The dotted line show the effect if there is an electron bite-out from 60 to 62 km, while the rest of the electron density profile follow the exponential variation. The broken line show the effect if the electron density has an electron bite-out and also a general reduction of density below 60 km height compared to the exponential variation.

We see that regardless of electron density profile the heating starts at around 55 km and that the height of the maximum heating and its value increase rapidly when the electron density is reduced. For moderate and decreasing electron densities the heating factor will increase with height throughout the PMWE heights and reach a maximum high up in the layer or above it. For such cases the maximum heating factor near the top of the PMWE height region can be in the range 8-10. For higher electron densities the maximum heating factor is found progressively lower down in height due to increased absorption of the heating transmission wave power in the lower region. For the case showed in Fig.2b with a maximum heating around 62 km, the maximum heating factor may be up to 3.5.

References [5,6] have developed a method, based on electron density irregularities being controlled by charged dust, by which one can estimate the heating factor from the ratio  $R1/R0$ . Here  $R0$  is the PMWE strength just before and  $R1$  just after the heater is switched on. The full formula includes the ratio of the background average electron density  $n_{e0}$  and ion density  $n_{i0}$  and is

$$T_{e,hot} = T_i \left( 1 + \frac{n_{i0}}{n_{e0}} - \sqrt{\frac{R1}{R0}} \right) / \left( \frac{n_{i0}}{n_{e0}} \sqrt{\frac{R1}{R0}} \right) \quad (1)$$

If the charge density on the dust is small compared to the electron density, the electron and ion density will be little affected (and there will be no electron bite-outs) and their ratio will be close to one. In such a case Eq.(1) reduces to

$$\frac{T_{e,hot}}{T_i} = \left( 2 - \sqrt{\frac{R1}{R0}} \right) / \sqrt{\frac{R1}{R0}} \quad (2)$$

Eq. 2 will overestimate the heating factor if the dust density is high so that  $n_{i0}/n_{e0} > 1$ .

In Fig.3 we show the observed heating factors as function of height for the PMWE's shown in Fig.1, determined by Eq.(2). We see that the heating apparently has a maximum in the height region 60-62 km and falls off above and below this. That the heating falls off with increasing height

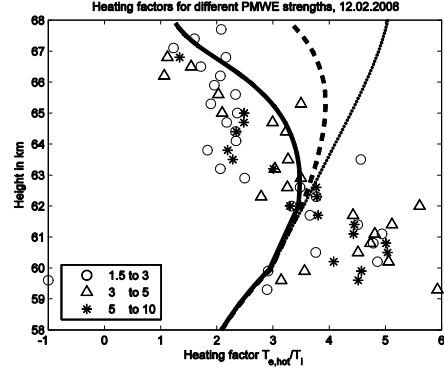


Fig.3. Observed heating factors determined by Eq.(2) are shown for the PMWE of Fig.1 for PMWE at different (Signal+Noise)/Noise strength intervals given in the box. The theoretical curve from Fig.2b, with electron bite-out at 60-62 km and a general reduction of electron density below 60 km is shown as a full line while the broken line corresponds to an electron density half of that for the full line and the dotted curve down to a fourth.

above ca 62 km is a clear indication that the electron density is high. This is to be expected, since the PMWE was observed under disturbed magnetospheric conditions. This is normally a requirement for having detectable PMWE. We have inserted the theoretical curve from Fig.2 where we have anticipated an electron bite-out at 60-62 km and assumed a lower electron density below 60 km than a pure exponential variation with height. We have also shown one case with a factor 0.5 and one with 0.25 lower electron density, to demonstrate the rapid change in the heating curve at these heights if the electron density change.

The first consequence of the observations in Fig.3 is that the rapid fall off with height above ~ 62 km show that the electron density is high and that a typical electron density at 65 km should be around  $n_e = 3 \times 10^9 \text{ m}^{-3}$ . This is also close to what Belova et al (2008) observed with the EISCAT VHF during PMWE conditions. The second is that the largest discrepancy between the theoretical curve and the observed values for the heating factor is in the height region 59.5-62 km where Eq.2 give too high values compared to the theoretical curves. This indicates that  $n_{i0}/n_{e0} > 1$  and that Eq.(1) should have been applied. Using a maximum value for the average heating factor of Fig.3 of 4.8, we find from Eq.(2) that this corresponds to

$R1/R0 \sim 0.12$ . Inserting this in Eq.(1) and demanding that  $T_{e,hot}/T_N$  should be reduced to  $\sim 3.5$ , we find that this requires that  $n_{i0}/n_{e0} \sim 3.1$ . These values are of course quite uncertain but they make it very probable that in the height region 59.5-62 km the dust charge density is high and comparable with that of the electrons. Studying Fig.1 we find that the height region where high dust charge density seem to be required coincides well with where we find the strongest and most extended PMWE structures. Based on our results these structures should have dust charge densities in excess of  $10^9 \text{ m}^{-3}$ . Since we expect that only a minor fraction of the dust particle in the PMWE have more than one negative unit charge, and that many are neutral [7], this indicates total dust densities of several times  $10^9 \text{ m}^{-3}$ .

#### 4. OBSERVED OVERSHOOT CHARACTERISTIC CURVES (OCC).

Reference [10] found that the average OCC curve over the one layer they examined, was characterized by a weak recovery and an overshoot by a factor of  $\sim 1.1$ . The heating factor was about 5 when averaged over 43 different OCC and height gates where  $(S+N)/N > 2$ . This is also probably too high but possibly only by a modest factor, if the electron density is somewhat

lower than in our case, since this layer was at 64 km height. In our case the PMWE in Fig.1 have 535, 293, 198, 132 and 21 OCC with  $(S+N)/N > 2, 3, 4, 5$  and 10 respectively. In Fig.4 we show the results where we have averaged the OCC curves over 8 different height and time segments. The 3 averaged OCC in the lower plots are from the 3 large structures seen in Fig.1. At each averaged OCC we have given the number of individual OCC and the heating cycle numbers which are included. For example in the lowest panel to the left this is the average of 37 individual OCC between heating cycles 41 to 60. The panels from bottom to top are for heights (58.7-61.7), (62-64.7) and (65-67.7) in km, respectively. We have also shown error bars as vertical red bars. The comparatively large error bars after the heater has been switched off may not be quite representative since they often are dominated by very few cases with large deviations from the average. A more careful selection of cycles to be included, for example by avoiding the cases where there is a rapid sinking or rising motion involved, where the signal can be strong in the early part of the cycle and practically disappear in the later parts of the cycle, may lead to considerably smaller errors. We see that the results in Fig.4 confirms that the heating factor is largest in the lower PMWE layers. The overshoot effect is present in practically all the curves, with the exception of the one in the upper panel to the left.

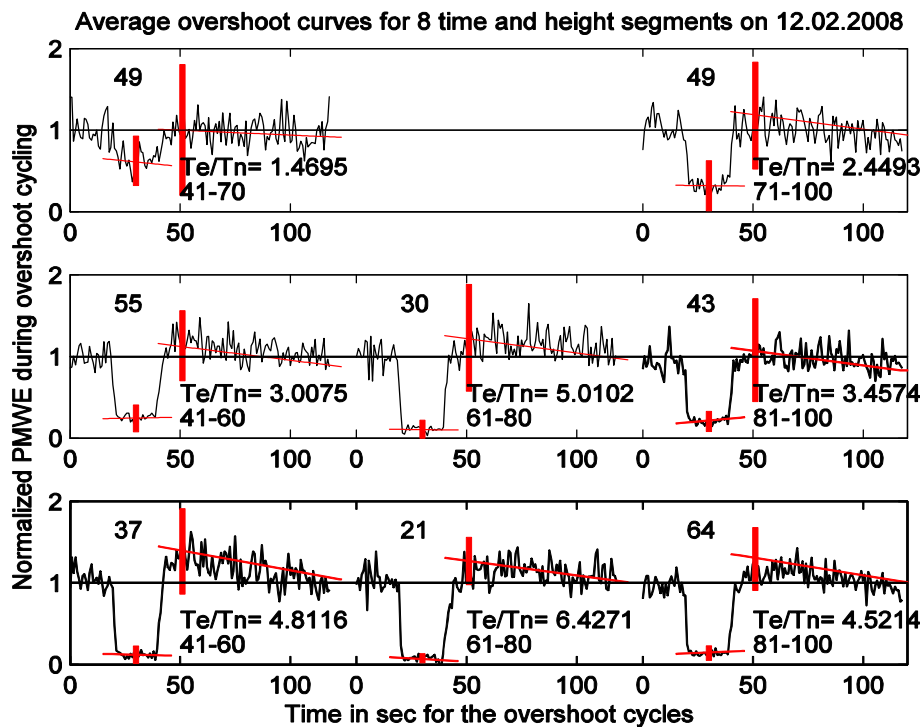


Figure 4. The results of averaging over many individual overshoot curves. For details see text.

The overshoot appear to become lower with increasing height, this is probably partly or wholly the result of the decrease in the heating factor but it can also be influenced by a reduction of dust size with height. It also appears that the relaxation time, the time for the PMWE signal to return to the undisturbed value, decreases with height. The relaxation time is around 70 sec in the low regions, decreasing to around 50-60 sec in the middle panel. If these differences are real they can also be an effect of decreasing dust sizes since the photodetachment effect, which appear to be needed to produce the relatively rapid relaxation [7], increase with decreasing dust size [16].

There are interesting differences between the overshoot curves as observed for PMSE [15,6] and the profiles we observe for the PMWE aside from the much lower intensity and smaller overshoots for the PMWE. Although the MORRO radar is not fully synchronized with the heater, causing a  $\pm 0.4$  sec uncertainty in our determination of the heater on and off times, it is clear that the behaviour of the signal after the heater is switched off, is characterized by an initial rapid recovery as for the PMSE but that this is followed by a much slower increase, resulting in a maximum signal from 10 to 30 sec after the heater has been switched off. In the phase where the heater is on there may be both a small recovery or a weakening of the signal. Although we have not fully explored how a difference in charging of the smallest and the larger PMWE dust particles can influence on the detailed structure of the overshoot curves we find it likely that for PMWE one must also consider a diffusion of its dust particles and how this is affected as the heater is switched on. If the dust diffuse to smooth the dust structures during the heating phase, this will compete with the extra charging of the dust and weaken the recovery, possibly causing a decrease of the signal as we sometimes see in Figure 4. This should also lead to a delayed recovery as we observe. When the heater is switched off the initial reaction is that the electrons cool and adjust rapidly, causing the “instantaneous” part of the overshoot while if the smoothed dust structures are reformed in a time 10-30 sec this may produce the delayed maximum.

## 5. CONCLUSIONS

Our observations of the heater modulated PMWE support that PMWE occur during periods of high electron densities in excess of  $10^9 \text{ m}^{-3}$  in the height region around 60 km. They also indicate that the total dust density can be high enough to influence on the electron and ion densities, leading to electron bite-outs of a similar nature as for PMSE. The large electron densities due to precipitation will normally lead to relatively modest heating factors not much more than 3-4 for PMWE below  $\sim 65$  km.

The overshoot is small but consistent and probably often a bit larger than the 1.1 factor reported by [10]. Details of the overshoot curve seem to require an explanation where some adjustments of the dust structures, caused by the heated electrons, also take place during and after the heating phase.

## REFERENCES

1. Rietveld, M. T., H. Kohl, and H. Kopka, Introduction to ionospheric heating at Tromsø. Part I: Experimental overview, *J. Atmos. Terr. Phys.*, 55, 577–599, 1993.
2. Chilson, P. B., E. Belova, M. T. Rietveld, S. Kirkwood, and U.-P. Hoppe, First artificially induced modulation of PMSE using the EISCAT heating facility. *Geophys. Res. Lett.*, 27, 3801–3804, 2000.
3. Havnes, O, Polar mesospheric summer echoes (PMSE) overshoot effect due to cycling of artificial electron heating, *J. Geophys. Res.*, 109, A02309, 2004. doi:10.1029/2003JA010159
4. Havnes, O., C. La Hoz, L. I. Næsheim, and M. T. Rietveld, First observations of the PMSE overshoot effect and its use for investigating the conditions in the summer mesosphere, *Geophys. Res. Lett.*, 30(23), 2229, 2003. doi:10.1029/2003GL018429
5. Havnes, O., La Hoz, C., Biebricher, A., Kassa, M., Meseret, T., Naesheim, L.I., and T. Zivkovic, Investigations of the mesospheric PMSE conditions by use of the new overshoot effect, *Phys. Scr.*, 107, 70-78, 2004.
6. Biebricher, A., O. Havnes, T. W. Hartquist, and C. La Hoz, On the influence of plasma absorption by dust on the PMSE overshoot effect, *Adv. Space Res.*, 38(11), 2541–2550, 2006.
7. Havnes; O and Kassa, M.: On the sizes and observable effects of dust particles in polar mesospheric winter echoes. *J. Geophys. Res.* 114, D09209, doi:10.1029/2008JD011276, 2009
8. Kavanagh, A.J., Honary, F., Rietveld, M.T., and A.Senior, First observations of the artificial modulation of polar mesosphere winter echoes. *Geophys. Res. Lett* 33, L19801, 2006. doi:10.1029/2006GL02756.

9. Belova, E., Smirnova, M., Rietveld, M.T., Isham, B., Kirkwood, S., and Siergienko, T, First observation of the overshoot effect for polar mesospheric winter echoes during radiowave electron temperature modulation, *Geophys. Res. Lett.*, 35, 2008. doi: [10.1029/2007GL032457](https://doi.org/10.1029/2007GL032457)
10. La Hoz., and O. Havnes, Artificial modification of polar mesospheric winter echoes with an RF heater: Do charged dust particles play an active role?, *J. Geophys. Res.*, 113, D19205, 2008. doi:10.1029/2008JD010460.
11. Kero, A., Enell, C.F., Kavanagh, A.J., Vierinen, J., Virtanen, I and Turunen, E, Could negative ion production explain the polar mesosphere winter echo (PMWE) modulation in active HF heating experiments? *Geophys. Res. Lett.*, 35, 23, L23102, 2008. Doi: 10.1029/2008GL035798
12. Zeller, O., Zecha, M., Bremer, J., Latteck, R and Singer, W.: Mean characteristics of mesospheric winter echoes at mid- and high latitudes. *J. Atmos. Solar-Terrestrial Phys.*, 68, 1087-1104, 2006.
13. Belova, E. G., A. B. Pashin, and W. B. Lyatsky, Passage of powerful HF radio wave through the ionosphere as a function of initial electron density profiles, *J. Atmos. Terr. Phys.*, 57, 265–272, 1995.
14. Kero, A., T. Bösinger, P. Pollari, E. Turunen, and M. Rietveld, First EISCAT measurements of electron-gas temperature in the artificially heated D-region ionosphere, *Ann. Geophys.*, 18, 1210–1215, 2000.
15. Kassa, M., O. Havnes, and E. Belova, The effect of electron bite-outs on artificial electron heating and the PMSE overshoot, *Ann. Geophys.*, 23, 1–11, 2005.
16. Weingartner, J.C., and B.T. Draine, Electron-ion recombination on grains and polycyclic aromatic hydrocarbons, *Astrophys. J.*, 563, 842-852, 2001.